Cureus Journal of Engineering

Open Access Original Article

Solvent-Free Particle Size Analysis of Fly Ash and Ground Granulated Blast Furnace Slag by Using Dry Accessory of Laser Diffraction Technique

Received 03/11/2025
Review began 03/25/2025
Review ended 04/15/2025
Published 05/21/2025

DOI: https://doi.org/10.7759/s44388-025-03686-x

Astha Jain [1]

1. Research & Technology Centre, Asian Paints Ltd, Navi Mumbai, IND

Corresponding author: Astha Jain, astha.jain@asianpaints.com

Abstract

Particle size measurement is one of the key parameters in controlling the properties of cement and supplementary cementitious materials (SCMs). Most commonly used technique for the particle size analysis of SCMs is sieve method. However, it does not provide the particle size distribution data (PSD) which is important to determine the mechanical properties of the mortar. Therefore, laser diffraction is one of the techniques to measure PSD of SCMs. Nowadays, laser light diffraction technique has become popular. Particle size analysis by laser diffraction technique, using wet method, is time-consuming as compared to dry method. Cementitious materials that undergo hydration cannot be analyzed by wet method with water as a dispersing media. In that case, organic solvent needs to be used as a dispersing media in wet method. Use of organic solvent leads to additional cost as well as environmental concerns. Therefore, a rapid, robust, and solvent free method has been developed by using Mastersizer, Aero S unit (dry accessory) of laser light diffraction technique for the determination of particle size of SCMs - Fly Ash (FA) & Ground Granulated Blast Furnace Slag (GGBS). The method was developed by analyzing samples at different pressure by using optimized parameters such as feed rate and hopper gap. Effect of pressure was observed on the particle size of FA, whereas the effect of pressure was not prominent on GGBS. The pressure was fixed at 3 barg for both the SCMs. By using the developed method, different samples of FA and GGBS were analyzed to check the particle size. It was found that the particle size (D50) of Fly Ash A - source 2 was 30.27 µ which is higher than the other FA samples. For other FA samples, D50 was approximately 19 µ. As per the ASTM specification, the max % > 45 µ for FA should be 34, which was not observed in the Fly ash A - source 2 sample. The % > 45 µ for FA - source 2 was 39.94. Similarly, for GGBS, the max % > 45 µ should be 20. For GGBS I, % > 45 µ was found to be 24.36, whereas for other GGBS J-source 1 and 2, maximum value was 13.48. As per the literature, a higher particle size will negatively affect the compressive strength of the mortar, whereas the use of finer SCMs with optimized size increases the mechanical properties equivalent to that of cement. The particle size analysis will help the formulators to use the SCMs of optimum particle size to get the desired compressive strength of mortars in the formulations. The study uses the sample in its powder form itself, which can be beneficial for the formulators to analyze SCMs which undergo hydration. The study presented here is not only environmentally friendly but also provides particle size data in no time to save time, energy, and resources.

Categories: Combustion and Alternative Fuels, Energy Efficiency and Conservation, Environmental and Sustainable Engineering
Keywords: supplementary cementitious materials (scms), compressive strength, environmental sustainability, ground granulated blast furnace slag, laser diffraction, particle size distribution, fly ash

Introduction

Concrete being present in large quantity and due to its lower cost, it is widely used in the construction industry. Concrete is majorly made up of three components: (1) cement, (2) aggregates - coarser and/or finer, and (3) water. Cement serves as a sturdy binder for buildings that holds steel, sand, and other coarser materials together. In the year 2022, India was second largest cement producer in the world. The predicted 370 million metric tons of cement produced in India represented 9% of the total cement produced worldwide in that year. The Indian cement market is dominated by private enterprises. Initiatives started by the Government of India such as “Housing for all” and “Smart city mission” aids the growth of the cement sector further. In Year 2023, the global concrete and cement market was valued, approximately, USD 439.06 billion and this is expected to increase with compound annual growth rate of 28.65% from year 2023 to 2032 [1]. However, use of cement is still a concern for the environment despite its versatility. Major concern during the production of cement is the release of CO_2, a greenhouse gas, during the conversion of limestone into lime. Reaction involved in the conversion process is given below [2]:

$$CaCO_3\ (s) \text{ -------> } CaO\ (s) + CO_2\ (g) \text{ ---------- (1)}$$

How to cite this article
Jain A (May 21, 2025) Solvent-Free Particle Size Analysis of Fly Ash and Ground Granulated Blast Furnace Slag by Using Dry Accessory of Laser Diffraction Technique. Cureus J Eng 2 : es44388-025-03686-x. DOI https://doi.org/10.7759/s44388-025-03686-x

Among all, cement industry is one of the largest sources of CO_2 emission. Approximately, 5-7% production of CO_2 is being contributed by the cement plants only. As per the reports, 900 kg CO_2 is emitted to the atmosphere for producing one ton of cement [3]. CO_2 is released during the calcination process where CaO is formed, which further reacts with silica, alumina, and iron rich raw materials to form clinker. Reactions involved in the manufacturing of cement is given below in Scheme 1 [4].

Scheme 1

1. Zone 1: 0-35 min, 800-1100°C

Decarbonation reaction

$CaCO_3$ (s) + Heat ------> CaO (s) + CO_2 (g)

2. Zone 2: 35-40 min, 1100-1300°C

Formation of secondary silicate phases

2CaO (s) + SiO_2 (s) + Heat ------> 2CaO. SiO_2 (s)

3. Zone 3: 40-50 min, 1300-1450-1300°C

Formation of ternary silicates and tetracalcium aluminoferrites

$2CaO.SiO_2$ (s) + CaO (s) + Heat --------> 3CaO. SiO_2 (s)

$3CaO.Al_2O_3$ (s) + CaO (s) + Fe_2O_3 (s) + Heat ---------> 4CaO.Al_2O_3.Fe_2O_3 (s)

4. Zone 4: 50-60 min, 1300-1000°C

Cooling and crystallization of various phases formed in the kiln.

Literature is available on the modification of cement production technology to reduce the emission of CO_2 associated with the production of cement. Reduction in emission of CO_2 from calcination process of limestone is the utmost challenging task. Calcination involves the formation of a substrate, CaO, which is a pre-requisite to form clinker minerals. Any modification in the calcination process can lead to a change in the mineral composition of the cement [5]. Therefore, research is being carried out in different areas as well. For example, the development of an eco-friendly cement, and the use of alternatives such as supplementary cementitious materials (SCMs) as a partial replacement of cement/clinker [6]. SCMs are the by-products from different industries [7] such as coal plants, steel plants, and others, and are discarded as waste without their maximum utilization, leading to landfills. Substitution of cement with SCMs reduces the cement consumption, and hence the emission of CO_2. Different type of SCMs which can be used to replace cement are Fly Ash (FA), Ground Granulated Blast Furnace Slag (GGBS), Blast Furnace Slag (BFS), Silica Fumes (SF), and others. According to ASTM C 681 [8], FA is further classified into two categories depending upon the type of coal used and its chemical composition: (1) Class C Fly Ash and (2) Class F Fly ash [9]. Properties such as flow and release of heat, $Ca(OH)_2$ consumption, bound water contents, compressive strength, and bulk resistivity [10] of cement-SCM mixture are affected by SCM reactivity and percentage of cement replaced [11]. For example, reactivity of SCM depends upon the chemical composition, phase, size, and morphology of its particles, specific surface area, percentage of SCM substituted, hardening conditions such as pH, temperature and cement type [12]. Characterization of SCMs is as important as it is for cement. Particle size, along with many other factors such as chemical composition, % substitution of SCM, morphology, and others, affects the compressive strength of the concrete mixture. SCMs are majorly divided into three categories, depending on the composition and reactivity [13]:

1. Pozzolanic material.

2. Hydraulic material.

3. Material showing inactivity or very small activity in cement system.

Manufacturing of cements with lower clinker contents favors the reduction of cement-industry-derived emissions [14]. Pozzolanic materials are siliceous and aluminous in nature which do not show self-

cementing properties. These materials either do not have or contain very less amount of calcium. However, to act as a cementitious material, reaction of pozzolans with $Ca(OH)_2$ in presence of water to form C-S-H (calcium-silicate-hydrate) and/or C-A-S-H (calcium-aluminate-silicate-hydrate) is crucial. Therefore, hydration of pozzolans is possible if they are mixed either with CaO or portland cement to form cementitious compounds such as C-S-H gel. Whereas hydraulic materials have enough calcium in their system and undergo hydration to form cementitious product without the need of any activator. Class C fly ash, BFS, and GGBS are a few examples of this class.

Hydration reaction of hydraulic material (cement) and pozzolanic material is given below:

Hydration reaction of cement

$C_3S + H_2O$ -------> C-S-H + $Ca(OH)_2$ + Heat ------ (2)

$C_2S + H_2O$ ---------> C-S-H + $Ca(OH)_2$+ Heat ------ (3)

$C_3A + H_2O$ ----------> C_3AH_6 + Heat ------ (4)

$C_4AF + H_2O$ ----------> C_3AH_6 + C-F-H + Heat ------ (5)

Hydration reaction of pozzolanic material is given below:

Pozzolans + $Ca(OH)_2 + H_2O$ --------> C-S-H gel ------ (6)

This C-S-H gel formed from the hydration reaction is also known as Tobermorite gel. Chemical formula along with their abbreviations is given below in Table *1*.

Chemical formula	Abbreviation used
3 $CaO.SiO_2$ (tricalcium silicate)	C_3S
2 CaO. SiO_2 (dicalcium silicate)	C_2S
3 CaO. Al_2O_3 (tricalcium aluminate)	C_3A
4 CaO. Al_2O_3. Fe_2O_3 (tetracalcium aluminoferrite)	C_4AF
3 CaO. $2SiO_2$. $3H_2O$ (calcium silicate hydrate)	C-S-H gel
3 CaO. Al_2O_3. $6H_2O$ (tricalcium aluminate hydrate)	C_3AH_6
CaO. Fe_2O_3. H_2O (calcium ferrite hydrate)	C-F-H

TABLE 1: Chemical Formula and Abbreviations Used for the Compounds Present in SCMs

SCM, supplementary cementitious material

Barbara Pacewsk et al. observed lower amount of bounded water and $Ca(OH)_2$ in cement-FA paste as compared to the control sample [12]. SCMs contain SiO_2 and Al_2O_3 which react with $Ca(OH)_2$, formed by the hydration reaction of cement, leading to more C-S-H and C-A-S-H bonds [13]. These cementitious (C-S-H and C-A-S-H) compounds are responsible for the development of strength of the concrete mixture. Bahed et al. reported that the substitution of ordinary portland cement (OPC) by FA enhanced the workability of the concrete as compared to the concrete without FA [15]. The workability of concrete in a FA substituted mixture is influenced by carbon content and fineness of FA [16]. Fineness property of SCM is very crucial for its reactivity to get desired strength of blended binders [17]. Pozzolanic reaction increases with the decrease in particle size and thus the hydration of cement by nucleation action. Surface of the fillers (SCMs) act as a nucleation site which can affect the hydration of the clinker [18]. According to literature, it has been found when particle size is high, it negatively affects the compressive strength of the concrete. To have good compressive strength, particle size of SCMs should be finer and lower than the particle size distribution (PSD) of the cement used [18]. Shaolong et al. also studied particle refinement effect and reported an increase in compressive strength from 38.0 MPa to 55.0 MPa when mean particle size (D50) of FA decreased from 26.4 to 1.5 μ for 30% FA-blended cement. He also observed when particle

size increased from 2.4 µ to 32.4 µ, compressive strength was drastically decreased [19]. Small particles of SCM can facilitate nucleation and growth of cement hydration products on the SCM surfaces, speeding up the early cement hydration and therefore the development of strength. Chindaprasirt et al. also reported that fineness of FA significantly affects the porosity and pore size of the paste and hence observed an increase in compressive strength with increase in fineness of SCMs [19,20]. However, after an optimum particle size, further decrease in particle size of SCMs can result to an increase in water demand of the concrete mixtures to get the desired workability [21]. Increase in water demand of the concrete mixture can deteriorate both strength and its durability [22]. Moreover, if particle size is decreased by grinding, this requires additional energy.

Teng et al. had reported when cement is substituted with GGBS, a decrease in permeability of concrete was observed due to decrease in pore size of cement [23]. As per ASTM standard, maximum % retention on 45 µ sieve for FA, should be 34 [8], whereas for Slag it is 20 [24]. To determine the fineness of cement, surface area is the most common property to be measured [25]. Measurement of surface area is an indispensable parameter but does not provide the actual particle size distribution. PSD data are considered to be of importance in determining the concrete performance [21]. Shaolong et al. described a relationship between compressive strength due to hydration of SCM with the particle size value. The relationship is given below in equation (7):

$$CHyd = b1\exp(-D/b2) \qquad \text{---------- (7)}$$

Where,

C_{Hyd} is the compressive strength due to hydration of SCM.

b1 and b2 are fitting coefficients

D is the D50 value of SCM particles

Therefore, it is important to control particle size of the SCMs which is being used to replace cement in the mixture. One of the limitations associated with the characterization of SCMs is the lack of specific standards for the determination of its physical properties. Characterization of SCM is being done by the methods which were specifically developed for cement analysis [21].

Techniques used for PSD measurement are image analysis, laser diffraction (LD), sieve analysis, and others. Particle size determination by image analysis requires careful analysis. Moreover, particle size by image analysis is a time-consuming process and needs experienced analyst to handle the same. Image analysis uses a small fraction of the sample which, sometimes, is not the representative of the whole sample. Thus, this cannot be implemented at production places for quality check (QC). Particle size analysis by LD method provides quick measurement, dynamic in nature, and it is user friendly. Particle size analyzer by LD technique works on the principle of diffraction of light. Light interacts with the particle and four different phenomena occurs:

(1) Reflection, (2) refraction, (3) absorption, (4) diffraction. Diffraction is the scattering of light from the edges of a particle. The diffracted light reaches the array of detectors located at different angles. This angular variation with the intensity of light is dependent on particle size and hence used to generate a scattering pattern. There are two optical models which are used to convert the scattering pattern into a particle size distribution graph: (1) Mie Model and (2) Fraunhofer Model. Mie model requires optical parameters of the sample and dispersing media. This gives more reliable results as absorption and refraction index of the particle are also taken into consideration which helps to calculate accurate results. However, as per the International Organization for Standardization (ISO) 13320, Fraunhofer can also be applied when particle size is more than 40 times the wavelength of light i.e. 25 µ. Fraunhofer model does not require optical parameters. Particle size analyzer has many applications, such as pharmaceutical industry, where dissolution of the drug, its effectiveness, and shelf life depend on it. It is also used in the food industries where texture and taste are affected by particle size. Along with that, particle size analysis is widely used by the cosmetics, paints, and inks, and plastic industries.

The LD technique, depending upon the nature of the material, can be used for the analysis in wet and dry mode. These two modes differ in the dispersion mechanism of a sample. Dry mode uses air as a dispersing media, whereas in wet mode a liquid media is used. For example, isopropyl alcohol, methanol, 0.1% sodium hexametaphosphate, and water are used for the dispersion of sample. Among many factors, for determination of particle size distribution by LD, accuracy of PSD data is dependent upon the proper dispersion of the sample. Arvaniti et al. worked on different techniques to measure the particle size of SCM and suggested the optical properties and dispersing media while using LD technique in wet mode [21]. One advantage of dry method over wet is the rapid analysis, reproducible results (when proper dispersion of the sample is achieved), a small amount of sample is required, no liquid media is required,

and hence there is a cost reduction associated with dispersing media. Moreover, required time of cleaning is insignificant compared to the wet mode.

The LD technique has some limitations too. This technique requires optical properties of the sample and dispersant. Therefore, new samples where the information about sample is not available cannot be analyzed by using LD method. Laser light diffraction assumes that all particles are perfectly spherical in nature. However, particles are not always spherical in nature which can underestimates the volume-based distribution of non-spherical particles. However, dry mode of LD technique can provide long-term benefits for the PSD measurement. Also, material undergoing hydration cannot be analyzed in wet method with water as a dispersing media.

The objective of this paper is to develop a robust method for the particle size analysis by using LD technique with dry mode for future prospects. We will discuss about the effect of pressure (bar gauge, barg) on particle size distribution data. Method for the determination of particle size was developed by optimizing the optical and mechanical parameters for FA and GGBS on dry accessory. Method was validated by performing parameters such as precision, intermediate precision, and robustness.

Materials And Methods

The development of method for particle size by using laser diffraction technique, dry mode, will be carried by using FA and GGBS from different sources and locations.

Geographical region of the SCM samples used in the experiment is given below in Table *2*.

Name of the SCM	Region
Fly Ash A (Source 1)	Western India
Fly Ash A (Source 2)	South India
Fly Ash A (Source 3)	Northern India
Fly Ash S	Westernmost India
GGBS R	Eastern India
GGBS I	Western India
GGBS J (Source 1)	Western India
GGBS J (Source 2)	Northwestern India

TABLE 2: Types of SCMs Used in the Analysis and its Geographical Regions

SCM, supplementary cementitious material; GGBS, Ground Granulated Blast Furnace Slag

Particle Size Analyser - Mastersizer 3000, Aero S unit was used for carrying out the experiments. For sample dispersion, ceramic venturi and general-purpose tray with hopper from Malvern Instruments, UK, were used (Figure *1*). The detection limit of the instrument is 0.01-3500 µ. Pressure range of the instrument is 0-4 barg. The laser used in the analysis is a combination of red and blue light. Source of red light is He-Ne laser with wavelength of 633 nm. Blue light is emitted by light emitting diode lamp with a wavelength of 470 nm. Dry accessory is attached with a vacuum and air compressor unit. During method development, hopper gap and feed rate was optimized.

Results

Method development for PSD analysis of fly ash

To carry out uniform and steady flow of the sample, hopper gap was initially fixed at a minimum value of 0.5 mm and feed rate at 30%. In subsequent experiments, hopper gap and feed rate was increased at the rate of 0.5 mm and 5%, respectively. It was found that at 0.5 mm hopper gap, when feed rate was increased at 5% from 30 to 90%, steady flow and the desired obscuration was not achieved. Therefore, hopper gap was increased to 1 mm. Sample flow was not uniform and desired obscuration was not achieved for a longer time even with 1 mm hopper gap and at 30% feed rate. As a result of this, feed rate at 5% was gradually increased. At 70% feed rate and 1 mm hopper gap, desired obscuration was achieved in the set measurement time of 5 s. After fixing the hopper gap, feed rate and measurement time of 5 s, pressure titration was carried out. For FA samples, Refractive Index (RI) and Absorption Index (AI) used was 1.56

and 1.00, respectively [26]. FA used for the method development is Fly Ash A (Source 1). Instrumental conditions used for the PSD analysis of FA are given below in Table 3.

Instrumental parameter	Instrumental condition
Hopper gap	1 mm
Feed rate	70%
Measurement time	5 s
Obscuration	0.1–6%
Analysis model	General mode
RI	1.56
Absorption Index	1.0
Pressure	1–4 barg

TABLE 3: Instrumental Conditions used for Fly Ash

RI, Refractive Index

At the set instrumental conditions, pressure titration was carried out to check the effect of pressure on the PSD of FA. Initially, pressure was fixed at 1.0 barg and the same sample was repeated six times to check the precision of the results. Similarly, at an interval of 1 barg, pressure titration was carried out from 1 barg to 4 barg. The same sample was analyzed six times at each pressure i.e. 1, 2, 3, and 4 barg. The PSD data of FA from pressure titration are given in Tables 15, 16, 17, and 18 of the appendices section. Fly Ash - Source 1 sample was analyzed by wet method as well. Sample was analyzed by using methanol as dispersing media and optical properties (RI and AI) were used as per Table 3. Mechanical parameters like stirring speed, sonication time, obscuration, and measurement time were used as per Reference [21]. Since, organic solvent was used, thermal gradients were also observed which are quite common with organic solvents. The thermal gradients could easily be identified as a large hump. Therefore, the results reported in the below table includes results from wet method (with and without thermal gradients). Results from the pressure titration, wet analysis, and sieve analysis are summarized in the below Table 4. Sieve analysis does not provide the particle size e.g. D(10), D(50), and D(90) values. It can provide the % retention of the particles. Therefore, only % < 45 µ value is given by sieve analysis. PSD graphs for FA by wet method, with and without thermal gradients are given in the (Figure 7) (a and b) respectively, of appendices section.

Average result (Dx in µ)	Dry method at pressure y (barg)				Wet method (with thermal gradients)	Wet method (without thermal gradients)	Sieve method
	1.0	2.0	3.0	4.0			
D_{10}	3.76	3.13	2.88	2.69	4.44	3.78	-
D_{50}	24.47	20.88	19.58	18.40	33.75	22.28	-
D_{90}	129.97	105.17	100.70	94.35	1149.00	100.78	-
% < 45 µ	66.16	70.72	72.32	74.09	56.48	69.29	84.00

TABLE 4: PSD Data of Fly Ash from Dry, Wet, and Sieve Method

PSD, particle size distribution

Graphical representation of PSD of FA at different pressures is given below Figure 1:

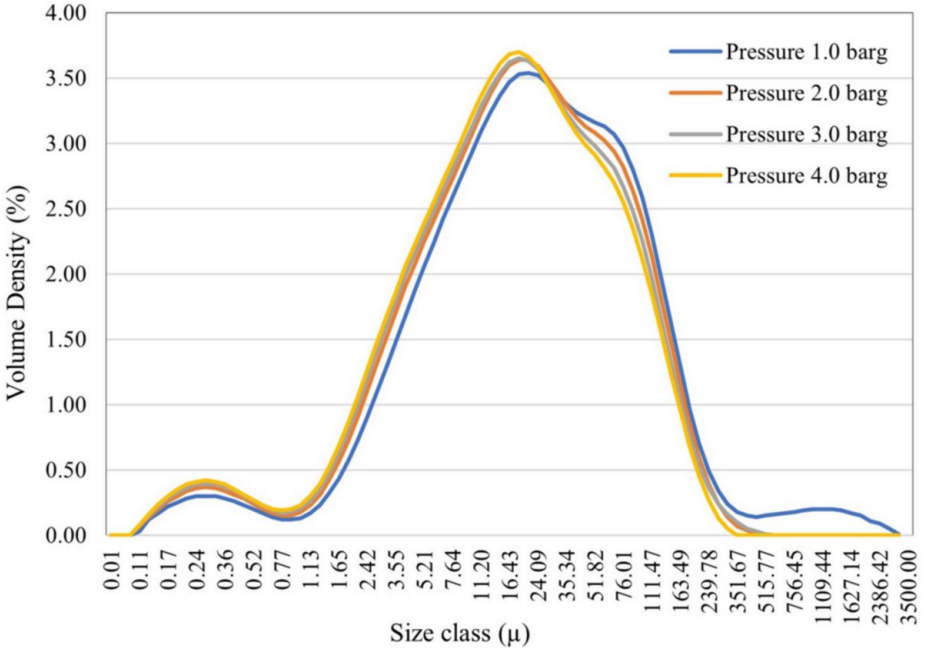

FIGURE 1: PSD Data of Fly Ash at Different Pressure

PSD, particle size distribution

Variation in D10, D50, D90 values with the change in pressure is shown below in Figure 2.

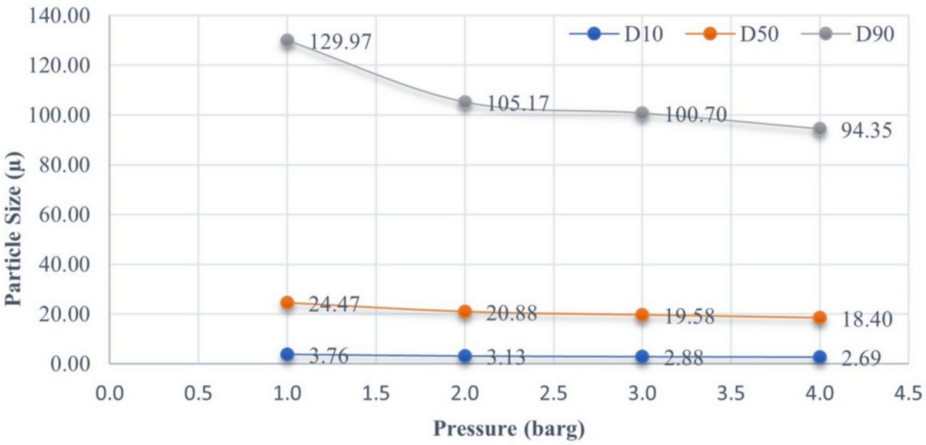

FIGURE 2: Effect of Pressure on D10, D50, and D90 Values of Fly Ash

As we increased the pressure, particle size decreased for FA sample. This is due to either breaking of primary particles or the proper dispersion of the sample got initiated. Maximum difference was found in D10 values when pressure changed from 1 to 2 barg. A small hump toward higher particle size region (around 1260 µ) was observed (Figure 1) when 1 barg pressure was used. This shows improper dispersion of the sample at lower pressure. Particle size variation was less when pressure was increased from 2 to 3 and then to 4 barg (Figure 2). % RSD was less than 5 when pressure changed in the range of 2 to 4 barg. Hence, 3 barg pressure was set for the analysis. A small hump toward finer side suggests that FA contains a small volume of finer particles as well. Final conditions used for the PSD analysis of FA are given below in Table 5. As per ISO 13320, relative standard deviation (RSD) for D50 should be less than or equal to 3%, and for D10 and D90, % RSD is 5 when mean particle size, D50, is > 10 µ. When D50 is <10, the % RSD values become double. However, for dry measurement the % RSD can be higher as every time new aliquot is used for the analysis.

Instrumental parameter	Instrumental condition
Hopper gap	1 mm
Feed rate	70%
Measurement time	5 s
Obscuration	0.1–6%
Analysis model	General mode
RI	1.56
Absorption index	1.0
Pressure	3 barg

TABLE 5: Final Instrumental Conditions for Fly Ash

RI, Refractive Index

(a) Precision of the method: Sample was analyzed nine times by Analyst 1 to check the repeatability of the method. Repeatability data is given in Table *19* in appendices.

(b) Robustness of the method was checked by performing two parameters:

(1). Intermediate precision: In this parameter, same sample was analyzed by two analyst and their % RSD was calculated. To check the robustness of the method, sample was analyzed by Analyst 2 as per the developed method. Total three runs were performed by using the same method. Cumulative data are given in Table *20* in appendices section.

Summarized values from intermediate precision are given below in Table *6*.

Value of	Fly ash A, source 1 pressure – 3.0 barg			
	Analyst 1	Analyst 2	Cumulative value (Analyst 1 and Analyst 2)	Cumulative %RSD
D_{10} (µm)	2.87	2.94	2.89	1.59
D_{50} (µm)	20.05	20.09	20.06	1.30
D_{90} (µm)	100.73	102.82	101.26	3.06
% < 45 µ	71.91	71.59	71.83	0.69

TABLE 6: Summarized Values of Fly Ash from Intermediate Precision

RSD, relative standard deviation

(2) Pressure change by 0.5 barg: Method robustness was checked by analyzing the sample at 2.5 and 3.5 barg. The change in set pressure by ± 0.5 barg. Results of the PSD data at 2.5 barg and 3.5 barg is given in Tables *21* and 22 in appendices section.

Summarized values from change in ±0.5 barg pressure are given below in Table *7*.

Pressure (barg)	Average result (Dx in μ)			% < 45 μ
	D_{10}	D_{50}	D_{90}	
2.5	2.99	20.14	103.35	71.56
3.0	2.88	19.58	100.70	72.32
3.5	2.79	18.93	96.37	73.32

TABLE 7: Summarized Values of Fly Ash from ±0.5 barg Pressure Change

It was found that with change in ± 0.5 barg, no significant change was observed.

%RSD was <5 for each value. Hence, method developed for the measurement of Fly Ash is a robust method.

Method development for PSD analysis of GGBS

To carry out uniform and steady flow of GGBS sample, method development started with fixing the hopper gap. It was initially fixed at 0.5 mm with feed rate of 30% which was again gradually increased upto 90%. Similar to FA, it was found that with 0.5 mm hopper gap, steady flow and the desired obscuration was not achieved. Therefore, hopper gap was increased to 1 mm. In the case of 1 mm hopper gap, with initial feed rate of 30%, sample flow was not uniform for a longer time. As a result of this, feed rate was gradually increased at 5%. At 45-50% feed rate, steady flow and desired obscuration was achieved at the set measurement time of 5 s. After fixing the hopper gap, feed rate and measurement time of 5 s, pressure titration was performed.

Method development for the PSD analysis of GGBS was carried out by using the parameters given in the Table *8* and pressure titration was carried out to check the effect of pressure on PSD of GGBS. GGBS used for the method development was GGBS R. The RI and AI used for the analysis of GGBS is 1.62 and 0.1, respectively [26]. Instrumental parameters for the PSD analysis of GGBS are given below in Table *8*.

Instrumental parameter	Instrumental condition
Hopper gap	1 mm
Feed rate	50%
Measurement time	5 s
Obscuration	0.1–6%
Analysis model	General mode
RI	1.62
Absorption index	0.1
Pressure	1.0-4.0 barg

TABLE 8: Instrumental Conditions Used for GGBS

RI, Refractive Index; GGBS, Ground Granulated Blast Furnace Slag

At given instrument conditions, pressure titration was carried out to check the effect of pressure on PSD of GGBS. Initially, pressure was fixed at 1.0 barg and six times same sample was analyzed to check the precision of the results. Afterwards, at an interval of 1.0 barg, pressure was increased upto 4.0 barg. Same sample was analyzed six times at each pressure. PSD results of GGBS R from pressure titration are given in Tables *23*, *24*, *25*, and 26 in the section appendices. Summarized D10, D50, and D90 values from pressure titration are given below in Table *9*. Results from the pressure titration are summarized in the below Table *9*.

Average result (Dx in μ)	Dry method at pressure y (barg)			
	1.0	2.0	3.0	4.0
D_{10}	3.27	2.90	2.71	2.59
D_{50}	20.82	20.20	19.56	19.20
D_{90}	52.99	52.05	51.84	51.06
% < 45 μ	84.07	84.68	85.07	85.63

TABLE 9: PSD Data for GGBS by Dry Method at Different Pressure

PSD, particle size distribution; GGBS, Ground Granulated Blast Furnace Slag

Graphical representation of PSD of GGBS at different pressures is given below Figure 3:

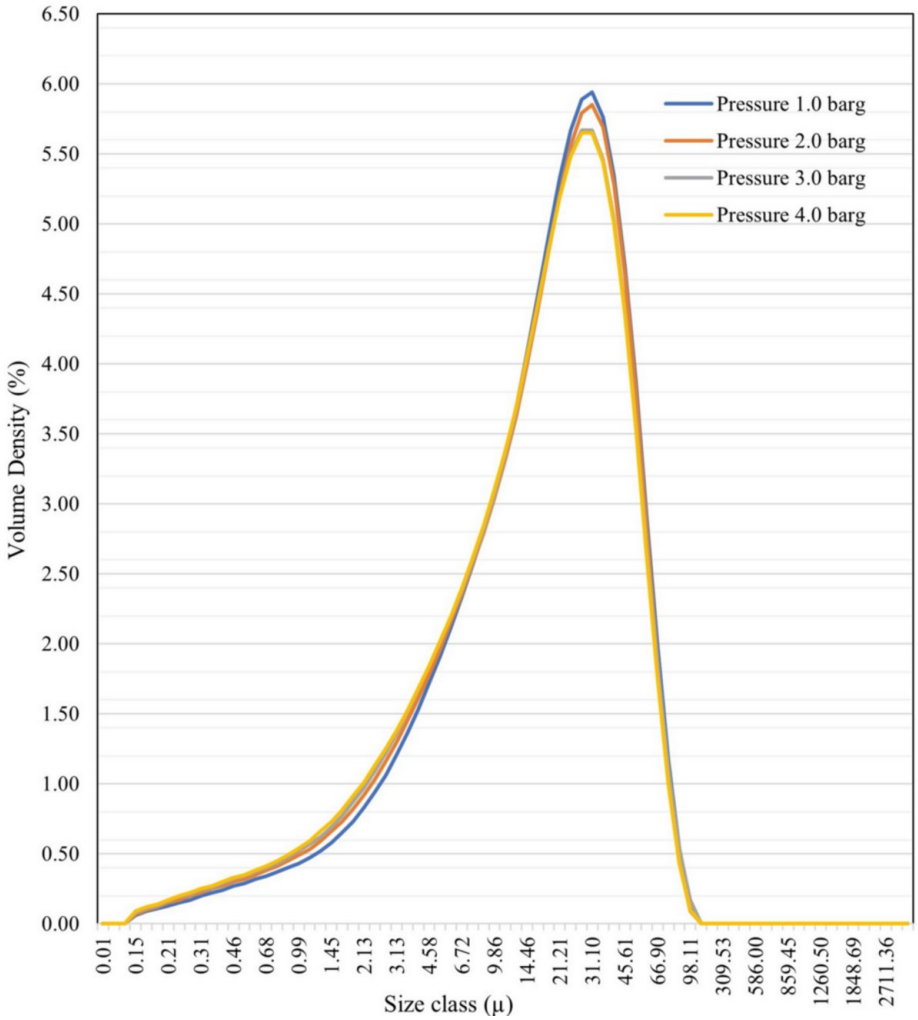

FIGURE 3: PSD Data of GGBS at Different Pressure

PSD, particle size distribution; GGBS, Ground Granulated Blast Furnace Slag

Change in D10, D50, and D90 values with the change in pressure is given below in Figure 4.

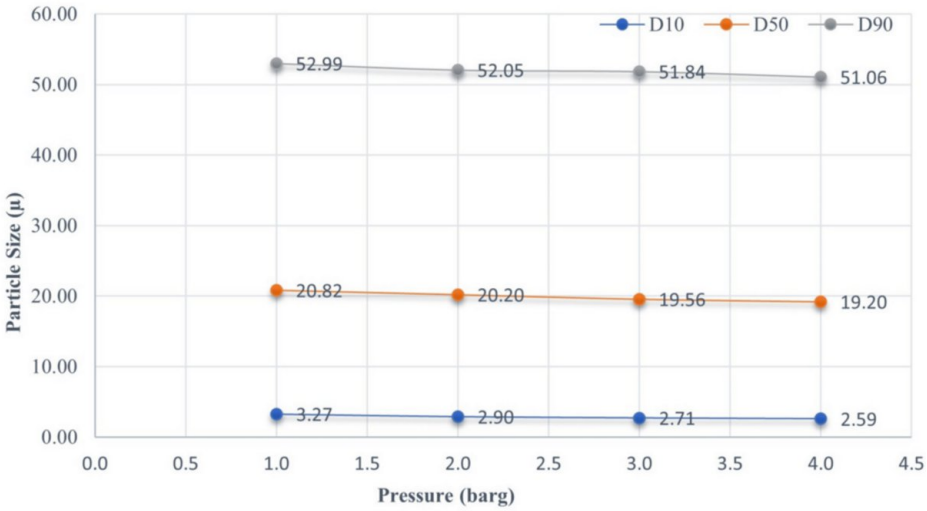

FIGURE 4: Effect of Pressure on D10, D50, and D90 Values of GGBS

GGBS, Ground Granulated Blast Furnace Slag

As we increased the pressure, particle size decreased for GGBS as well. Maximum difference was found in D10 values when pressure changed from 1 to 2 barg. This suggests that at lower pressure sample was not dispersed properly. No change was observed in the nature of PSD graph of GGBS at any pressure (Figure *3*). Particle size variation was less when pressure was increased in the range of 2 to 4 barg (Figure *4*). Observed %RSD was less than 5 when pressure varied in between 2 and 4 barg. Hence, 3 barg pressure was fixed for the analysis. Final instrumental conditions for the PSD analysis of GGBS are given below in Table *10*.

Instrumental parameter	Instrumental condition
Hopper gap	1 mm
Feed rate	50%
Measurement time	5 s
Obscuration	0.1–6%
Analysis model	General mode
RI	1.62
Absorption index	0.1
Pressure	3 barg

TABLE 10: Final Instrumental Conditions for GGBS

GGBS, Ground Granulated Blast Furnace Slag; RI, Refractive Index

(a) Precision of the method: Sample was analyzed nine times by Analyst 1 to check the repeatability of the method. Repeatability data at the developed method is given in Table *27* of appendices section.

(b) Robustness: Robustness was performed as per the previous section by calculating intermediate precision and varying the pressure by ±0.5 barg.

(1). Intermediate Precision: To check robustness of the method, sample was analyzed by Analyst 2 as per the developed method. Total three runs were performed by using the same method.

Cumulative data after performing intermediate precision is given in Table *28*

Summarized values of GGBS from intermediate precision are given below in Table 11.

Value of	GGBS R, pressure – 3.0 barg			
	Analyst 1	Analyst 2	Cumulative value (Analyst 1 and Analyst 2)	Cumulative %RSD
D_{10} (µm)	2.73	2.73	2.73	0.79
D_{50} (µm)	19.93	19.59	19.85	0.91
D_{90} (µm)	52.36	52.05	52.28	0.57
% < 45 µ	84.67	84.94	84.74	0.24

TABLE 11: Summarized Values of GGBS from Intermediate Precision

GGBS, Ground Granulated Blast Furnace Slag; RSD, relative standard deviation

(2). Change in pressure by 0.5 barg: To further check robustness of the method, pressure was changed by ±0.5 barg. Particle size results were studied at 2.5 barg and 3.5 barg. Results are given in Table 29 and 30 of appendices. Summarized values from change in ±0.5 barg pressure of GGBS are given below in Table 12.

Pressure (barg)	Average result (Dx in µ)			% < 45 µ
	D_{10}	D_{50}	D_{90}	
2.5	2.80	19.83	51.96	84.91
3.0	2.71	19.56	51.84	85.07
3.5	2.66	19.35	51.49	85.33

TABLE 12: Summarized Values of GGBS from ±0.5 barg Pressure Change

GGBS, Ground Granulated Blast Furnace Slag

PSD analysis of fly ash and GGBS from different sources and locations

Here, three samples of FA and GGBS from different sources (refer Table 2) were analyzed by using the developed method.

Fly Ash A (source 1) and GGBS R, both samples were used for the method development process. Hence, PSD analysis for these two samples has not been repeated in this section.

(1). Determination of Particle Size of FA: Particle size analysis of fly ash A (source 2), fly ash A (source 3) and fly ash S from different sources and locations was done by using the conditions given in Table 5. All the three samples of FA were analyzed three times and % RSD was found to be <5. PSD data of FA from different sources/locations are given in Table 31 of appendices section.

Results for FA samples by dry method are summarized in below Table 13.

Name and source of SCM	D_{10} (µm)	D_{50} (µm)	D_{90} (µm)	% < 45 µ
Fly Ash A - Source 2	4.10	30.27	154.51	60.06
Fly Ash A - Source 3	2.77	19.05	94.71	73.46
Fly Ash S	2.47	19.00	124.14	70.67

TABLE 13: PSD Data of Fly Ash from Different Sources and Locations

SCM, supplementary cementitious material; PSD, particle size distribution

Graphical representation of D10, D50, and D90 values of FA from different locations is given below in Figure 5.

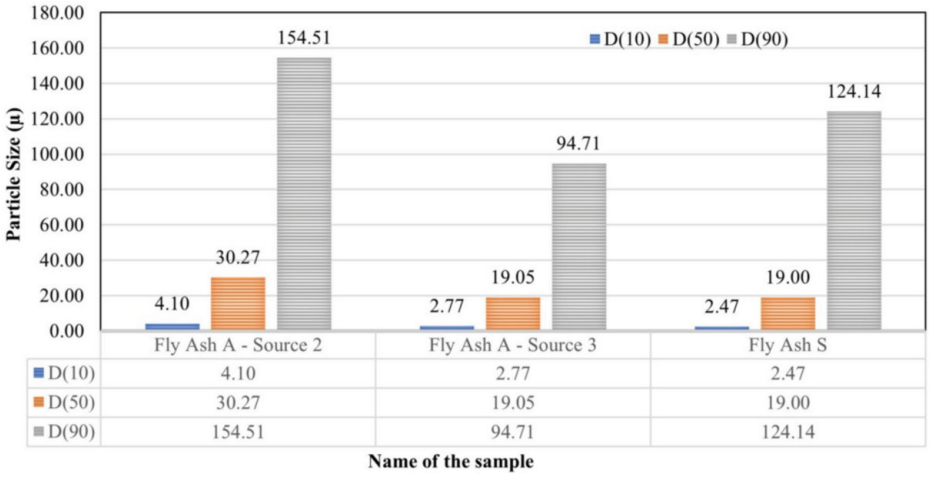

FIGURE 5: PSD Data of Fly Ash from Different Locations

PSD, particle size distribution

From the above data, it is concluded that Fly Ash A - source 2 has a higher particle size as compared to all the other three samples including Fly Ash A from source 1. Whereas D10 and D50 values are similar for Fly Ash A from source 3 and Fly Ash S. Hence, it can be concluded that the PSD data of all the three samples except Fly Ash A - source 2 are similar to each other. Reactivity of SCM depends upon the chemical composition, phase, size and morphology of its particles, specific surface area, percentage of SCM substituted, hardening conditions such as pH, temperature and cement type [12].

(2). Determination of Particle Size of GGBS: Particle size analysis of GGBS I, GGBS J (source 1), and GGBS (source 2) from different sources and locations (refer Table 2) was done by using the conditions given in Table 10. All the three samples of GGBS were analyzed three times and %RSD was reported for each sample. Results are given in Table 32.

Results of PSD data for GGBS samples are summarized below in Table 14.

Name and source of SCM	D_{10} (µm)	D_{50} (µm)	D_{90} (µm)	% < 45 µ
GGBS I	1.00	7.84	107.06	75.64
GGBS J Source 1	2.95	17.19	51.18	86.52
GGBS J Source 2	2.91	14.69	38.28	94.03

TABLE 14: D10, D50, and D90 Values of GGBS from Different Locations and Sources

SCM, supplementary cementitious material; GGBS, Ground Granulated Blast Furnace Slag

Graphical representation of D10, D50, and D90 values of GGBS from different locations is given below in Figure *6*.

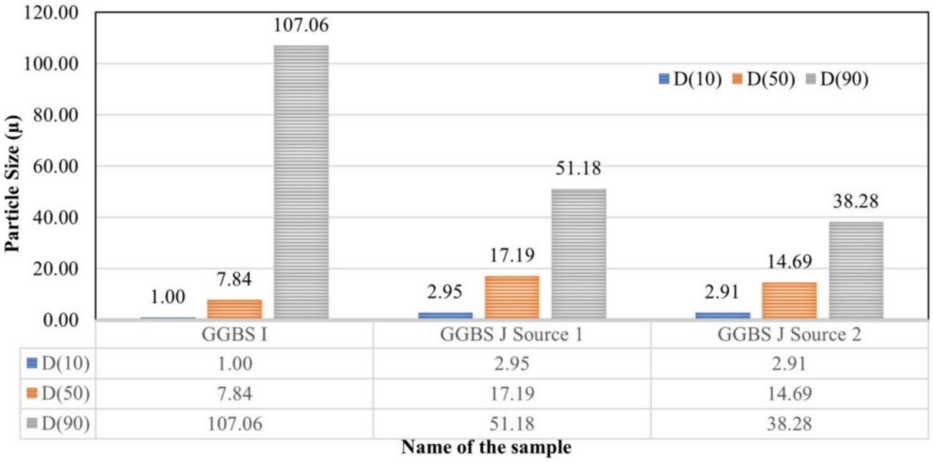

FIGURE 6: PSD Data of GGBS from Different Locations

GGBS, Ground Granulated Blast Furnace Slag; PSD, particle size distribution

From the above data, it is concluded that GGBS I has a finer particle size and larger span as compared to GGBS J source 1 and GGBS J source 2. D10 values of GGBS J from both the locations are similar but varied in their D50 and D90. It can be concluded that SCMs from same source can also be varied in their particle size. Among all the four samples of GGBS (GGBS R, GGBS I, GGBS J - source 1 and 2), GGBS I was an outlier and GGBS J from source 2 was found to be finer than GGBS R and GGBS J - source 1. Fineness property of SCM is very crucial for its reactivity to get desired strength of blended binders [17]. Shaolong et al. also studied particle refinement effect and reported an increase in compressive strength from 38.0 MPa to 55.0 MPa when mean particle size (D50) of FA decreased from 26.4 to 1.5 µ for 30% FA-blended cement [19]. Optimum particle size of SCMs is very crucial, as further decrease in particle size of SCMs can result to an increase in water demand of the concrete mixtures to get the desired workability [21]. Increase in water demand of the concrete mixture can deteriorate both strength and durability [22]. It was observed that reactivity of natural pozzolans increased when particle size decreased [27].

Discussion

As we increased the pressure, particle size decreased for FA sample. This is due to either breaking of primary particles or proper dispersion of the sample got initiated. Maximum difference was found in D10 values when pressure changed from 1 to 2 barg. A small hump toward higher particle size region (around 1260 µ) was observed (Figure *1*) when 1 barg pressure was used. This shows improper dispersion of the sample at lower pressure. Particle size variation was less when pressure was increased from 2 to 3 and then to 4 barg (Figure *2*). % RSD was less than 5 when pressure changed in the range of 2 to 4 barg. Hence, 3 barg pressure was set for the analysis. A small hump toward finer side suggests that FA contains a small volume of finer particles as well. FA samples were analyzed by wet method with methanol as a dispersing media. Use of organic solvents tends to give, sometimes, thermal gradients which can easily be observed as a large hump. The thermal gradients can subside gradually with the time of analysis. Presence of thermal gradients tend to change the actual particle size. Therefore, thermal gradients are not acceptable in any distribution graph. Particle size distribution for FA with and without thermal gradient is shown in

the Figure 7a and b, respectively. Particle size by wet method and dry method is comparable. Conventional sieve analysis does not provide the particle size values (e.g. D10, D50, and D90), which play a crucial role in determining the mechanical properties of a concrete mixture.

For GGBS, as we increased the pressure, particle size decreased for GGBS as well. Maximum difference was found in D10 values when pressure changed from 1 to 2 barg. This suggests that at lower pressure sample was not dispersed properly. No change was observed in the nature of PSD graph of GGBS at any pressure (Figure 3). Particle size variation was less when pressure was increased in the range of 2 to 4 barg (Figure 4). Observed % RSD was less than 5 when pressure varied in between 2 and 4 barg. Hence, 3 barg pressure was fixed for the analysis.

From the data given in Table 13, it is concluded that Fly Ash A - source 2 has a higher particle size as compared to all the other three samples including Fly Ash A from source 1. Whereas D10 and D50 values are similar for Fly Ash A from source 3 and Fly Ash S. Hence, it can be concluded that PSD data of all the three samples except Fly Ash A - source 2 are similar to each other (refer Figure 5).

From the data given in Table 14, it is concluded that GGBS I has finer particle size and larger span as compared to GGBS J source 1 and GGBS J source 2. D10 values of GGBS J from both the locations are similar but varied in their D50 and D90 values. It can be concluded that SCMs from same source can also be varied in their particle size.

Among all the four samples of GGBS (GGBS R, GGBS I, GGBS J - source 1 and 2), GGBS I was an outlier and GGBS J from source 2 was found to be finer than GGBS R and GGBS J - source 1 (refer Figure 6).

Conclusions

A quick, robust, and environment-friendly method has been developed for the particle size analysis of SCMs such as FA and GGBS. The method was developed by changing the feed rate and hopper gap to get a steady flow of the sample. Constant flow of sample was observed when hopper gap was fixed at 1 mm for both FA and GGBS with feed rate of 70% and 50%, respectively. Pressure titration was carried out to study the effect of pressure on the particle size distribution of FA. Difference in particle size was insignificant when analyzed at 2, 3, and 4 barg pressure. Therefore, mean value of 2, 3, 4 barg i.e. 3 barg was fixed for FA. Pressure titration was carried out for GGBS as well to study the effect of pressure on particle size. It was observed that the nature of frequency distribution graph was same at all the pressures. However, the % difference between two consecutive pressures such as at 1 and 2 barg, was higher as compared to the difference observed at 2, 3, and 4 barg pressure. Therefore, 3 barg pressure was fixed for the particle size measurement of GGBS. Robustness of the method was checked by performing the analysis at 3.0 ± 0.5 barg pressure for both the SCMs where observed %RSD was ≤5. Method was validated by a different analyst where %RSD of intermediate precision was ≤5.

Particle size by wet method and dry method was comparable. Conventional sieve method is time consuming and does not provide the distribution of particle size, e.g. D10, D50, and D90. These values play a significant role in determining the mechanical properties of a concrete mixture. Therefore, due to sustainability, cost efficiency, and rapid analysis, it is recommended to use dry method for the particle size analysis of SCMs.

Appendices

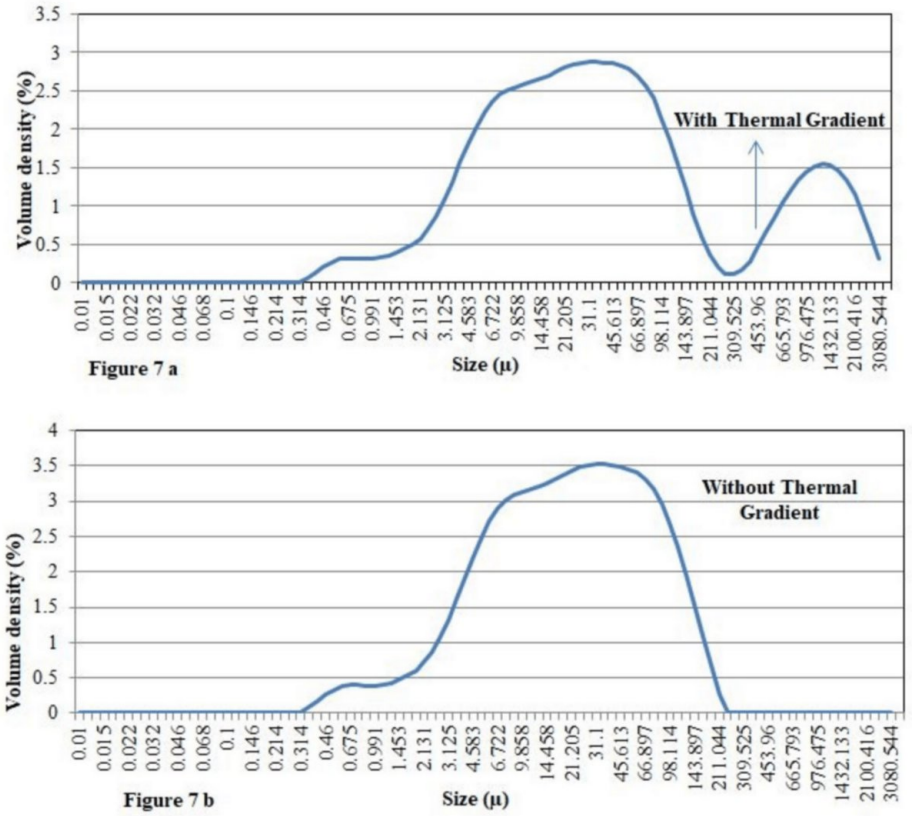

FIGURE 7: PSD Data of Fly Ash by Wet Method With and Without Thermal Gradients

PSD, particle size distribution

Run No.	Average result (Dx in µ)			% < 45 µ
	D_{10}	D_{50}	D_{90}	
RUN 1	3.68	23.84	121.91	67.05
RUN 2	3.84	24.27	125.05	66.48
RUN 3	3.80	25.16	136.67	65.33
RUN 4	3.70	24.00	124.58	66.70
RUN 5	3.88	25.69	148.23	64.51
RUN 6	3.67	23.85	123.38	66.88
Mean	3.76	24.47	129.97	66.16
%RSD	2.35	3.16	8.00	1.53

TABLE 15: PSD Data of Fly Ash at 1.0 barg Pressure

PSD, particle size distribution

Run No.	Average result (Dx in μ)			% < 45 μ
	D_{10}	D_{50}	D_{90}	
RUN 1	3.14	20.76	103.72	70.95
RUN 2	3.14	21.02	105.38	70.57
RUN 3	3.15	20.93	105.37	70.69
RUN 4	3.08	20.69	105.01	70.94
RUN 5	3.15	21.03	107.01	70.39
RUN 6	3.14	20.85	104.52	70.80
Mean	3.13	20.88	105.17	70.72
%RSD	0.92	0.67	1.04	0.31

TABLE 16: PSD Data of Fly Ash at 2.0 barg Pressure

PSD, particle size distribution

RUN No.	Average result (Dx in μ)			% < 45 μ
	D_{10}	D_{50}	D_{90}	
RUN 1	2.88	19.45	98.61	72.63
RUN 2	2.87	19.51	100.92	72.37
RUN 3	2.89	19.52	101.44	72.27
RUN 4	2.86	19.76	102.25	72.06
RUN 5	2.88	19.64	100.54	72.22
RUN 6	2.89	19.62	100.45	72.36
Mean	2.88	19.58	100.70	72.32
%RSD	0.39	0.58	1.21	0.27

TABLE 17: PSD Data of Fly Ash at 3.0 barg Pressure

PSD, particle size distribution

RUN No.	Average result (Dx in μ)			% < 45 μ
	D_{10}	D_{50}	D_{90}	
RUN 1	2.68	18.26	93.46	74.29
RUN 2	2.69	18.45	95.14	73.96
RUN 3	2.70	18.44	94.00	74.08
RUN 4	2.69	18.22	92.15	74.48
RUN 5	2.73	18.55	95.79	73.77
RUN 6	2.68	18.47	95.58	73.92
Mean	2.69	18.40	94.35	74.09
%RSD	0.65	0.70	1.50	0.35

TABLE 18: PSD Data of Fly Ash at 4.0 barg Pressure

PSD, particle size distribution

	RUN No.	D_{10} (μm)	D_{50} (μm)	D_{90} (μm)	% < 45 μ
Pressure – 3.0 barg fly ash A – source 1	RUN 1	2.94	20.36	102.36	71.52
	RUN 2	2.82	19.67	95.72	72.60
	RUN 3	2.86	20.29	104.38	71.48
	RUN 4	2.90	20.22	102.30	71.73
	RUN 5	2.86	20.00	98.86	72.13
	RUN 6	2.86	20.09	102.88	71.64
	RUN 7	2.85	19.75	97.60	72.43
	RUN 8	2.89	20.17	101.53	71.69
	RUN 9	2.85	19.95	100.95	71.95
	Mean	2.87	20.05	100.73	71.91
	%RSD	1.23	1.17	2.77	0.56

TABLE 19: Precision Data of Fly Ash

	RUN No.	D_{10} (µm)	D_{50} (µm)	D_{90} (µm)	% < 45 µ
Fly ash A source 1 pressure – 3.0 barg (Analyst 1)	RUN 1	2.94	20.36	102.36	71.52
	RUN 2	2.82	19.67	95.72	72.60
	RUN 3	2.86	20.29	104.38	71.48
	RUN 4	2.90	20.22	102.30	71.73
	RUN 5	2.86	20.00	98.86	72.13
	RUN 6	2.86	20.09	102.88	71.64
	RUN 7	2.85	19.75	97.60	72.43
	RUN 8	2.89	20.17	101.53	71.69
	RUN 9	2.85	19.95	100.95	71.95
	Mean	2.87	20.05	100.73	71.91
	%RSD	1.23	1.17	2.77	0.56
Pressure – 3.0 barg (Analyst 2)	RUN 1	2.97	20.50	106.93	70.75
	RUN 2	2.94	20.05	102.77	71.73
	RUN 3	2.92	19.73	98.77	72.28
	MEAN	2.94	20.09	102.82	71.59
	%RSD	0.74	1.94	3.97	1.08
Cumulative mean		2.89	20.06	101.26	71.83
Cumulative %RSD		1.59	1.30	3.06	0.69

TABLE 20: Intermediate Precision Data of Fly Ash

RUN No.	Average result (Dx in µ)			% < 45 µ
	D_{10}	D_{50}	D_{90}	
RUN 1	3.01	20.24	104.31	71.39
RUN 2	2.99	19.96	100.85	72.00
RUN 3	2.97	20.08	103.51	71.54
RUN 4	2.98	20.18	103.80	71.53
RUN 5	2.99	20.21	102.99	71.54
RUN 6	2.98	20.19	104.67	71.34
Mean	2.99	20.14	103.35	71.56
%RSD	0.42	0.52	1.32	0.32

TABLE 21: PSD Data of Fly Ash at 2.5 barg Pressure

PSD, particle size distribution

RUN No.	Average result (Dx in μ)			% < 45 μ
	D_{10}	D_{50}	D_{90}	
RUN 1	2.77	18.90	95.53	73.48
RUN 2	2.80	18.71	96.73	73.32
RUN 3	2.75	18.72	94.41	73.70
RUN 4	2.79	18.95	96.68	73.36
RUN 5	2.79	19.02	97.00	73.17
RUN 6	2.82	19.26	97.90	72.92
Mean	2.79	18.93	96.37	73.32
%RSD	0.83	1.09	1.27	0.36

TABLE 22: PSD Data of Fly Ash at 3.5 barg Pressure

PSD, particle size distribution

RUN No.	Average result (Dx in μ)			% < 45 μ
	D_{10}	D_{50}	D_{90}	
RUN 1	3.28	20.73	53.34	83.98
RUN 2	3.28	20.81	53.01	84.06
RUN 3	3.29	20.89	53.19	83.94
RUN 4	3.29	20.96	53.40	83.83
RUN 5	3.24	20.67	51.71	84.73
RUN 6	3.26	20.87	53.27	83.90
Mean	3.27	20.82	52.99	84.07
%RSD	0.59	0.51	1.21	0.40

TABLE 23: PSD Data of GGBS at 1.0 barg Pressure

PSD, particle size distribution; GGBS, Ground Granulated Blast Furnace Slag

RUN No.	Average result (Dx in μ)			% < 45 μ
	D_{10}	D_{50}	D_{90}	
RUN 1	2.88	20.20	52.03	84.66
RUN 2	2.90	20.15	52.33	84.59
RUN 3	2.89	20.14	52.28	84.59
RUN 4	2.90	20.24	52.06	84.63
RUN 5	2.89	20.18	51.63	84.89
RUN 6	2.91	20.27	51.99	84.68
Mean	2.90	20.20	52.05	84.68
%RSD	0.33	0.26	0.48	0.13

TABLE 24: PSD Data of GGBS at 2.0 barg Pressure

PSD, particle size distribution; GGBS, Ground Granulated Blast Furnace Slag

RUN No.	Average result (Dx in μ)			% < 45 μ
	D_{10}	D_{50}	D_{90}	
RUN 1	2.74	19.58	51.73	85.14
RUN 2	2.72	19.58	51.96	84.98
RUN 3	2.71	19.56	51.79	85.10
RUN 4	2.71	19.55	51.89	85.06
RUN 5	2.70	19.56	51.84	85.06
RUN 6	2.69	19.52	51.86	85.05
Mean	2.71	19.56	51.84	85.07
%RSD	0.63	0.10	0.16	0.06

TABLE 25: PSD Data of GGBS at 3.0 barg Pressure

PSD, particle size distribution; GGBS, Ground Granulated Blast Furnace Slag

RUN No.	Average result (Dx in μ)			% < 45 μ
	D_{10}	D_{50}	D_{90}	
RUN 1	2.60	19.26	51.11	85.55
RUN 2	2.58	19.18	51.09	85.58
RUN 3	2.59	19.25	51.37	85.45
RUN 4	2.55	19.04	50.27	86.13
RUN 5	2.60	19.30	51.26	85.49
RUN 6	2.60	19.16	51.27	85.56
Mean	2.59	19.20	51.06	85.63
%RSD	0.72	0.50	0.79	0.29

TABLE 26: PSD Data of GGBS at 4.0 barg Pressure

PSD, particle size distribution; GGBS, Ground Granulated Blast Furnace Slag

	RUN No.	D_{10} (μm)	D_{50} (μm)	D_{90} (μm)	% < 45 μ
GGBS R pressure – 3.0 barg	RUN 1	2.73	20.03	52.08	84.78
	RUN 2	2.76	20.05	52.66	84.48
	RUN 3	2.71	19.85	52.20	84.79
	RUN 4	2.73	19.92	52.22	84.72
	RUN 5	2.75	19.94	52.57	84.57
	RUN 6	2.75	19.98	52.48	84.59
	RUN 7	2.71	19.86	52.34	84.71
	RUN 8	2.71	19.83	52.27	84.74
	RUN 9	2.73	19.93	52.43	84.65
	Mean	2.73	19.93	52.36	84.67
	%RSD	0.70	0.40	0.36	0.12

TABLE 27: Precision Data of GGBS

GGBS, Ground Granulated Blast Furnace Slag

	RUN No.	D_{10} (µm)	D_{50} (µm)	D_{90} (µm)	% < 45 µ
GGBS R pressure – 3.0 barg (Analyst 1)	RUN 1	2.73	20.03	52.08	84.78
	RUN 2	2.76	20.05	52.66	84.48
	RUN 3	2.71	19.85	52.20	84.79
	RUN 4	2.73	19.92	52.22	84.72
	RUN 5	2.75	19.94	52.57	84.57
	RUN 6	2.75	19.98	52.48	84.59
	RUN 7	2.71	19.86	52.34	84.71
	RUN 8	2.71	19.83	52.27	84.74
	RUN 9	2.73	19.93	52.43	84.65
	Mean	2.73	19.93	52.36	84.67
	%RSD	0.70	0.40	0.36	0.12
Pressure – 3.0 barg (Analyst 2)	RUN 1	2.74	19.51	51.77	85.12
	RUN 2	2.76	19.76	52.60	84.57
	RUN 3	2.69	19.50	51.78	85.14
	MEAN	2.73	19.59	52.05	84.94
	%RSD	1.22	0.75	0.92	0.38
Cummulative mean		2.73	19.85	52.28	84.74
Cummulative %RSD		0.79	0.91	0.57	0.24

TABLE 28: PSD Data of GGBS with Intermediate Precision

PSD, particle size distribution; GGBS, Ground Granulated Blast Furnace Slag

RUN No.	Average result (Dx in µ)			% < 45 µ
	D_{10}	D_{50}	D_{90}	
RUN 1	2.84	19.98	52.46	84.64
RUN 4	2.80	19.75	51.53	85.16
RUN 5	2.80	19.79	51.84	84.96
RUN 6	2.79	19.75	52.25	84.82
RUN 7	2.79	19.77	51.44	85.21
RUN 8	2.79	19.94	52.26	84.65
Mean	2.80	19.83	51.96	84.91
%RSD	0.68	0.52	0.82	0.29

TABLE 29: PSD Data of GGBS at 2.5 barg Pressure

PSD, particle size distribution; GGBS, Ground Granulated Blast Furnace Slag

RUN No.	Average result (Dx in μ)			% < 45 μ
	D_{10}	D_{50}	D_{90}	
RUN 1	2.65	19.35	51.58	85.29
RUN 2	2.68	19.37	51.61	85.26
RUN 3	2.64	19.30	51.44	85.38
RUN 4	2.66	19.35	51.22	85.48
RUN 5	2.68	19.42	51.66	85.20
RUN 6	2.65	19.30	51.47	85.37
Mean	2.66	19.35	51.49	85.33
%RSD	0.63	0.24	0.31	0.12

TABLE 30: PSD Data of GGBS at 3.5 barg Pressure

PSD, particle size distribution; GGBS, Ground Granulated Blast Furnace Slag

Source name	RUN No.	D_{10} (μm)	D_{50} (μm)	D_{90} (μm)	% < 45 μ
Fly Ash A (Source 2)	RUN 1	4.16	30.85	155.97	59.59
	RUN 2	4.10	30.42	154.69	59.89
	RUN 3	4.05	29.53	152.87	60.71
	Mean	4.10	30.27	154.51	60.06
	%RSD	1.44	2.22	1.01	0.96
Fly Ash A (Source 3)	RUN 1	2.77	19.35	95.72	73.12
	RUN 2	2.72	18.84	93.51	73.66
	RUN 3	2.81	18.97	94.91	73.60
	Mean	2.77	19.05	94.71	73.46
	%RSD	1.66	1.39	1.18	0.41
Fly Ash S	RUN 1	2.53	19.57	126.96	70.02
	RUN 2	2.42	18.84	120.21	70.99
	RUN 3	2.45	18.61	125.25	71.00
	Mean	2.47	19.00	124.14	70.67
	%RSD	2.33	2.65	2.83	0.80

TABLE 31: PSD Data of Fly Ash from Different Sources and Locations

PSD, particle size distribution

Source name	RUN No.	D_{10} (µm)	D_{50} (µm)	D_{90} (µm)	% < 45 µ
GGBS I	RUN 1	1.02	7.81	105.91	76.29
	RUN 2	1.00	7.82	104.46	75.77
	RUN 3	0.99	7.90	110.83	74.85
	Mean	1.00	7.84	107.06	75.64
	%RSD	1.28	0.58	3.12	0.96
GGBS J Source 1	RUN 1	2.95	17.21	51.37	86.41
	RUN 2	2.95	17.18	51.23	86.49
	RUN 3	2.94	17.19	50.92	86.65
	Mean	2.95	17.19	51.18	86.52
	%RSD	0.14	0.10	0.45	0.14
GGBS J Source 2	RUN 1	2.93	14.72	38.36	93.99
	RUN 2	2.91	14.67	38.24	94.03
	RUN 3	2.90	14.69	38.24	94.08
	Mean	2.91	14.69	38.28	94.03
	%RSD	0.53	0.18	0.18	0.05

TABLE 32: GGBS Data from Different Sources and Locations

GGBS, Ground Granulated Blast Furnace Slag

Additional Information

Author Contributions

All authors have reviewed the final version to be published and agreed to be accountable for all aspects of the work.

Concept and design: Astha Jain

Acquisition, analysis, or interpretation of data: Astha Jain

Drafting of the manuscript: Astha Jain

Critical review of the manuscript for important intellectual content: Astha Jain

Supervision: Astha Jain

Disclosures

Human subjects: All authors have confirmed that this study did not involve human participants or tissue. **Animal subjects:** All authors have confirmed that this study did not involve animal subjects or tissue. **Conflicts of interest:** In compliance with the ICMJE uniform disclosure form, all authors declare the following: **Payment/services info:** All authors have declared that no financial support was received from any organization for the submitted work. **Financial relationships:** All authors have declared that they have no financial relationships at present or within the previous three years with any organizations that might have an interest in the submitted work. **Other relationships:** All authors have declared that there are no other relationships or activities that could appear to have influenced the submitted work.

Acknowledgements

The author would like to thank the Asian Paints Management for their support in publishing this work. The author also thanks Dr. Amit Joshi, Dr. Chandrashekara Haramagatti, Dr. Girish Mirchandani, and Dr. Venugopal Raghavendra for their valuable suggestions. The author also acknowledges the support given

by Mrs. Sushma Ray that was required during the research.

References

1. Concrete and Cement Market Size, Share, Growth, and Industry Analysis, By Type (Concrete, Cement), By Application (Residential Sector, Industrial Sector, Commercial Sector), and Regional Insights and Forecast To 2032. (2025). Accessed: March 11, 2025: https://www.businessresearchinsights.com/market-reports/concrete-and-cement-market-117747.
2. Gibbs MJ, Soyka P, Conneely D: CO2 emissions from cement production. Good Practice Guidance and Uncertainty Management in National Greenhouse Gas Inventories. 2000, 176.
3. Benhelal E, Zahedi G, Shamsaei E, Bahadori A: Global strategies and potentials to curb CO2 emissions in cement industry. Journal of Cleaner Production. 2013, 51:142-61. 10.1016/j.jclepro.2012.10.049
4. Lavagna L, Nisticò R: An insight into the chemistry of cement—a review. Applied Sciences. 2022, 13:203. 10.3390/app13010203
5. Scrivener KL, John VM, Gartner EM: Eco-efficient cements: potential economically viable solutions for a low-CO2 cement-based materials industry. Cement and Concrete Research. 2018, 114:2-26. 10.1016/j.cemconres.2018.03.015
6. Miller SA, John VM, Pacca SA, Horvath A: Carbon dioxide reduction potential in the global cement industry by 2050. Cement and Concrete Research. 2018, 114:115-24. 10.1016/j.cemconres.2017.08.026
7. Siddique R, Khan MI: Supplementary Cementing Materials. Springer, Berlin; 2011. 10.1007/978-3-642-17866-5
8. Standard specification for coal fly ash and raw or calcined natural pozzolan for use in concrete. Accessed: March 14, 2023: https://store.astm.org/c0618-22.html.
9. Bhatt A, Sharon P, Mohanakrishnan AA, Abri A, Sattler M, Techapaphawit S: Physical, chemical, and geotechnical properties of coal fly ash: a global review. Case Studies in Construction Materials. 2019, 11:e00263. 10.1016/j.cscm.2019.e00263
10. Ramanathan S, Croly M, Suraneni P: Comparison of the effects that supplementary cementitious materials replacement levels have on cementitious paste properties. Cement and Concrete Composites. 2020, 112:103678. 10.1016/j.cemconcomp.2020.103678
11. Qu Z, Liu Z, Si R, Zhang Y: Effect of various fly ash and ground granulated blast furnace slag content on concrete properties: experiments and modelling. Materials. 2022, 15:3016. 10.3390/ma15093016
12. Pacewska B, Wilińska I: Usage of supplementary cementitious materials: advantages and limitations. Journal of Thermal Analysis and Calorimetry. 2020, 142:371-93. 10.1007/s10973-020-09907-1
13. Kurdowski W: Cement and Concrete Chemistry. Springer Nature, 2014. 10.1007/978-94-007-7945-7
14. Sierra OM, Payá J, Monzó J, Borrachero MV, Soriano L, Quiñonez J: Characterization and reactivity of natural pozzolans from Guatemala. Applied Sciences. 2022, 12:11145. 10.3390/app122111145
15. Bahedh MA, Jaafar MS: Ultra high-performance concrete utilizing fly ash as cement replacement under autoclaving technique. Case Studies in Construction Materials. 2018, 9:e00202. 10.1016/j.cscm.2018.e00202
16. Raghav M, Park T, Yang HM, Lee SY, Karthick S, Lee HS: Review of the effects of supplementary cementitious materials and chemical additives on the physical, mechanical and durability properties of hydraulic concrete. Materials. 2021, 14:7270. 10.3390/ma14237270
17. Celik IB: The effects of particle size distribution and surface area upon cement strength development. Powder Technology. 2009, 188:272-76. 10.1016/j.powtec.2008.05.007
18. Scrivener KL, Lothenbach B, De Belie N, Gruyaert E, Skibsted J, Snellings R, Vollpracht A: TC 238-SCM: hydration and microstructure of concrete with SCMs. Materials and Structures. 2015, 48:835-62. 10.1617/s11527-015-0527-4
19. Liu S, Zhang T, Guo Y, Wei J, Yu Q: Effects of SCMs particles on the compressive strength of micro-structurally designed cement paste: inherent characteristic effect, particle size refinement effect, and hydration effect. Powder Technology. 2018, 330:1-11. 10.1016/j.powtec.2018.01.087
20. Chindaprasirt P, Jaturapitakkul C, Sinsiri T: Effect of fly ash fineness on compressive strength and pore size of blended cement paste. Cement and Concrete Composites. 2005, 27:425-28. 10.1016/j.cemconcomp.2004.07.003
21. Arvaniti EC, Juenger MCG, Bernal SA, et al.: Physical characterization methods for supplementary cementitious materials. Materials and Structures. 2014, 48:3675-86. 10.1617/s11527-014-0430-4
22. Scrivener KL, Kirkpatrick RJ: Innovation in use and research on cementitious material. Cement and Concrete Research. 2008, 38:128-36. 10.1016/j.cemconres.2007.09.025
23. Teng S, Lim TYD, Divsholi BS: Durability and mechanical properties of high strength concrete incorporating ultra fine Ground Granulated Blast-furnace Slag. Construction and Building Materials. 2013, 40:875-81. 10.1016/j.conbuildmat.2012.11.052
24. ASTM C989-09, Standard Specification for Slag Cement for Use in Concrete & Mortars. ASTM International. Accessed: March 5, 2024: https://store.astm.org/c0989_c0989m-24.html.
25. Stark U, Mueller A: Particle size distribution of cements and mineral admixtures—standard and sophisticated measurements. 11th International Congress on the Chemistry of Cement (ICCC), 11-16 May 2003. Grieve G, Owens G (ed): Durban, South Africa; 2003.
26. Jewell RB, Rathbone RF: Optical properties of coal combustion byproducts for particle-size analysis by laser diffraction. Coal Combustion and Gasification Products. 2009, 1:1-6. 10.4177/ccgp-d-09-00001
27. Skibsteda J, Snellings R: Reactivity of supplementary cementitious materials (SCMs) in cement blends. Cement and Concrete Research. 2019, 124:105799. 10.1016/j.cemconres.2019.105799